

1 **An antisense RNA capable of modulating the
2 expression of the tumor suppressor microRNA-34a**
3

4 **Jason T. Serviss^{1*}, Felix Clemens Richter^{1,2}, Nathanael Johansson
5 Andrews¹, Miranda Houtman, Laura Schwarzmüller, Per Johnsson,
6 Jimmy Van Den Eynden, Erik Larsson³, Dan Grandér¹, Katja Pokrovskaia
7 Tamm¹**

8
9 ¹ Department of Oncology and Pathology, Karolinska Institutet, Stockholm,
10 Sweden

11 ² Kennedy Institute of Rheumatology, University of Oxford, Roosevelt Drive,
12 Oxford OX3 7FY, UK

13 ³Department of Medical Biochemistry and Cell Biology, Institute of
14 Biomedicine, The Sahlgrenska Academy, University of Gothenburg, SE-405
15 30 Gothenburg, Sweden

16 *** Correspondence:**

17 Jason T. Serviss, Department of Oncology and Pathology, Karolinska
18 Institutet, Stockholm, Sweden, SE-17177. jason.serviss@ki.se

21 **Abstract**

23 The microRNA-34a is a well-studied tumor suppressor microRNA (miRNA)
24 that is a direct down-stream target of TP53 and has roles in multiple pathways
25 associated with oncogenesis, such as proliferation, cellular growth, and
26 differentiation. Due to its wide variety of targets that suppress oncogenesis, it
27 is not surprising that miR34a expression has been shown to be dys-regulated
28 in a wide variety of both solid tumors and hematological malignancies.
29 Despite this, the mechanisms by which miR34a is regulated in these cancers
30 is not well studied. Here we find that the *miR34a* antisense RNA, a long non-
31 coding RNA transcribed antisense to *miR34a*, is critical
32 for *miR34a* expression and mediation of its cellular functions in multiple types
33 of human cancer. In addition, we characterize miR34a asRNA's ability to
34 facilitate miR34a expression under multiple types of cellular stress in both
35 TP53 deficient and wild-type settings.

36 **Introduction**

37 In recent years advances in functional genomics has revolutionized our
38 understanding of the human genome. Evidence now points to the fact that
39 approximately 75% of the genome is transcribed but only ~1.2% of this is
40 responsible for encoding proteins (International Human Genome Sequencing
41 2004, Djebali et al. 2012). Of these recently identified elements, long non-
42 coding (lnc) RNAs are defined as transcripts exceeding 200bp in length with a
43 lack of a functional open reading frame. Some lncRNAs are dually classified
44 as antisense (as) RNAs that are expressed from the same locus as a sense
45 transcript in the opposite orientation. Current estimates using high-throughput
46 transcriptome sequencing, indicate that up to 20-40% of the approximately
47 20,000 protein-coding genes exhibit antisense transcription (Chen et al. 2004,
48 Katayama et al. 2005, Ozsolak et al. 2010). The hypothesis that asRNAs play
49 an important role in oncogenesis was first proposed when studies increasingly
50 found examples of aberrant expression of these transcripts and other lncRNA
51 subgroups in tumor samples (Balbin et al. 2015). Although studies
52 characterizing the functional importance of asRNAs in cancer are limited to
53 date, characterization a number of individual transcripts has led to the
54 discovery of multiple examples of asRNA-mediated regulation of several well
55 known tumorigenic factors (Yap et al. 2010, Johnsson et al. 2013). The
56 mechanisms by which asRNAs accomplish this are diverse, and include
57 recruitment of chromatin modifying factors (Rinn et al. 2007), acting as
58 microRNA (miRNA) sponges (Memczak et al. 2013), and causing
59 transcriptional interference (Conley et al. 2012).

60

61 Responses to cellular stress, e.g. DNA damage, sustained oncogene
62 expression, and nutrient deprivation, are all tightly monitored and orchestrated
63 cellular pathways that are commonly dys-regulated in cancer. Cellular
64 signaling in response to these types of cellular stress often converge on the
65 transcription factor *TP53* that regulates transcription of coding and non-coding
66 downstream targets. One non-coding target of *TP53* is the tumor suppressor
67 microRNA known as *miR34a* (Raver-Shapira et al. 2007).
68 Upon *TP53* activation *miR34a* expression is increased allowing it to down-
69 regulate its targets involved in cellular pathways such as, growth factor
70 signaling, apoptosis, differentiation, and cellular senescence (Lal et al. 2011,
71 Slabakova et al. 2017). *miR34a* is a crucial factor in mediating activated *TP53*
72 response and it is often deleted or down-regulated in human cancers and has
73 also been shown to be a valuable prognostic marker (Cole et al. 2008,
74 Gallardo et al. 2009, Zenz et al. 2009, Cheng et al. 2010, Liu et al. 2011).
75 Reduced *miR34a* transcription has been shown to be mediated via epigenetic
76 regulation in many solid tumors, such as colorectal-, pancreatic-, and ovarian
77 cancer (Vogt et al. 2011), as well as multiple types of hematological
78 malignancies (Chim et al. 2010). In addition, *miR34a* has been shown to be
79 transcriptionally regulated via *TP53* homologs, *TP63* and *TP73*, other
80 transcription factors, e.g. *STAT3* and *MYC*, and, in addition, post-
81 transcriptionally through miRNA sponging by the *NEAT1* lncRNA (Chang et al.
82 2008, Su et al. 2010, Agostini et al. 2011, Rokavec et al. 2015, Ding et al.
83 2017). Despite these findings, the mechanisms underlying *miR34a* regulation
84 in the context of oncogenesis have not yet been fully elucidated.

85

Studies across multiple cancer types have reported a decrease in oncogenic phenotypes when miR34a expression is induced in a p53-null background, although endogenous mechanisms for achieving this have not yet been discovered (Liu et al. 2011, Ahn et al. 2012, Yang et al. 2012, Stahlhut et al. 2015, Wang et al. 2015). In addition, previous reports have identified a lncRNA originating in the antisense orientation from the miR34a locus which is regulated by TP53 and is induced upon cellular stress (Rashi-Elkeles et al. 2014, Hunten et al. 2015, Leveille et al. 2015, Ashouri et al. 2016, Kim et al. 2017). Despite this, none of these studies have continued to functionally characterize this transcript. In this study we functionally characterize the *miR34a* asRNA transcript, and find that modulating the levels of the *miR34a* asRNA is sufficient to increase levels of *miR34a* and results in a decrease of multiple tumorigenic phenotypes. Furthermore, we find that *miR34a* asRNA-mediated up-regulation of *miR34a* is sufficient to induce endogenous cellular mechanisms counteracting several types of stress stimuli in a *TP53* deficient background. Finally, similar to the functional roles of antisense transcription at protein-coding genes, we find that antisense RNAs are also capable of regulating cancer-associated miRNAs.

104

105 **Results**

106

107 ***miR34a* asRNA is a broadly expressed, non-coding transcript whose**
108 **levels correlate with *miR34a* expression**

109

110 *miR34a* asRNA is transcribed in a “head-to-head” orientation with
111 approximately 100 base pair overlap with the *miR34a* host gene (HG) (**Fig.**
112 **1a**). Due to the fact that sense/antisense pairs can be both concordantly and
113 discordantly expressed, we sought to evaluate this relationship in the case of

114 *miR34a* HG and its asRNA. Using a diverse panel of cancer cell lines, we
115 detected co-expression of both the *miR34a* HG and *miR34a* asRNA (**Fig. 1b**).
116 We included *TP53*+/+, *TP53* mutated, and *TP53*-/- cell lines in the panel due
117 to previous reports that *miR34a* is a known downstream target of TP53.
118 These results indicate that *miR34a* HG and *miR34a* asRNA are co-expressed
119 and that their expression levels correlate with *TP53* status, with *TP53*-/- cell
120 lines tending to have decreased expression of both transcripts.

121

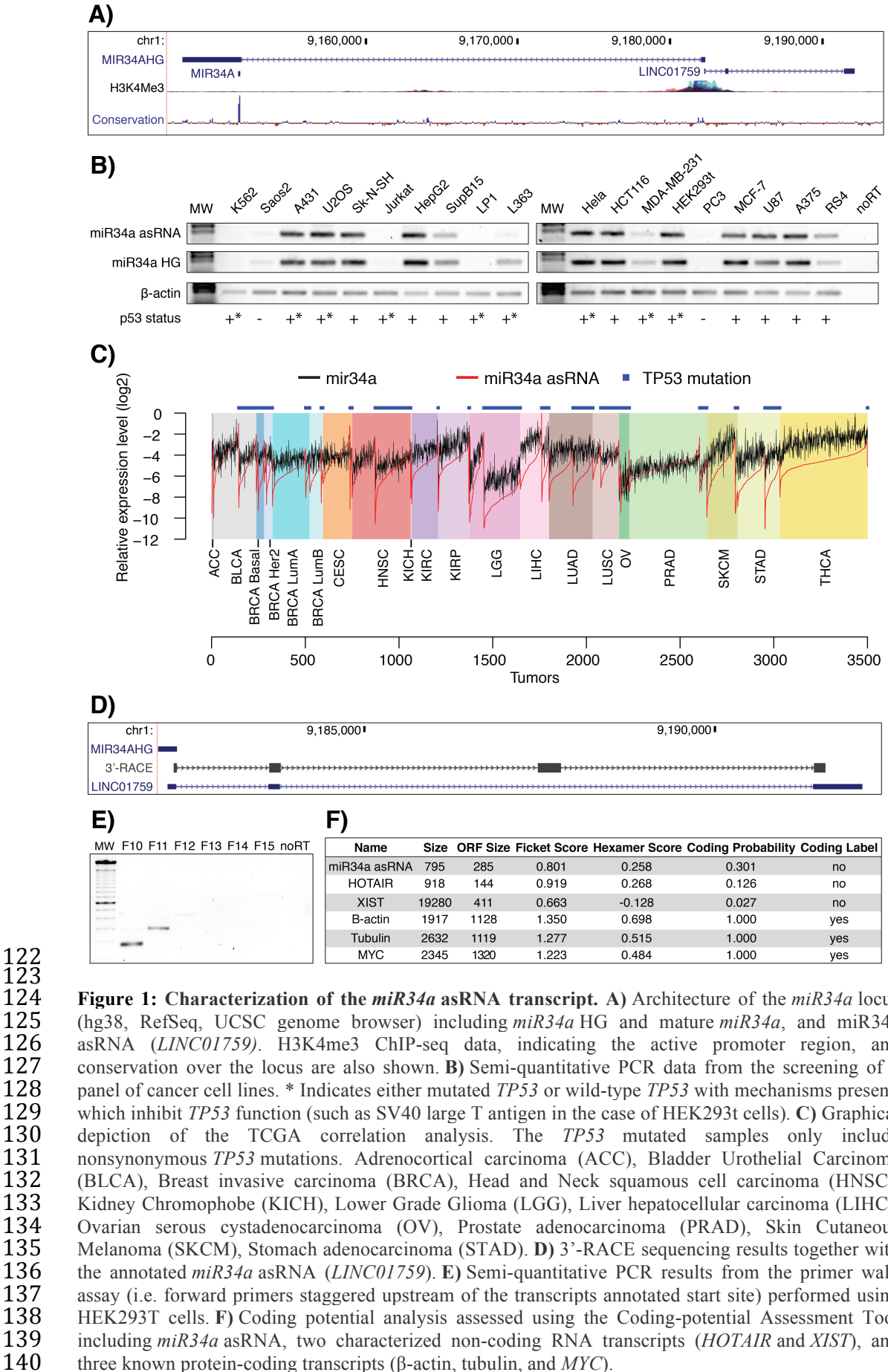


Figure 1: Characterization of the *miR34a* asRNA transcript. A) Architecture of the *miR34a* locus (hg38, RefSeq, UCSC genome browser) including *miR34a* HG and mature *miR34a*, and *miR34a* asRNA (*LINC01759*). H3K4me3 ChIP-seq data, indicating the active promoter region, and conservation over the locus are also shown. B) Semi-quantitative PCR data from the screening of a panel of cancer cell lines. * Indicates either mutated *TP53* or wild-type *TP53* with mechanisms present, which inhibit *TP53* function (such as SV40 large T antigen in the case of HEK293t cells). C) Graphical depiction of the TCGA correlation analysis. The *TP53* mutated samples only include nonsynonymous *TP53* mutations. Adrenocortical carcinoma (ACC), Bladder Urothelial Carcinoma (BLCA), Breast invasive carcinoma (BRCA), Head and Neck squamous cell carcinoma (HNSC), Kidney Chromophobe (KICH), Lower Grade Glioma (LGG), Liver hepatocellular carcinoma (LIHC), Ovarian serous cystadenocarcinoma (OV), Prostate adenocarcinoma (PRAD), Skin Cutaneous Melanoma (SKCM), Stomach adenocarcinoma (STAD). D) 3'-RACE sequencing results together with the annotated *miR34a* asRNA (*LINC01759*). E) Semi-quantitative PCR results from the primer walk assay (i.e. forward primers staggered upstream of the transcripts annotated start site) performed using HEK293T cells. F) Coding potential analysis assessed using the Coding-potential Assessment Tool including *miR34a* asRNA, two characterized non-coding RNA transcripts (*HOTAIR* and *XIST*), and three known protein-coding transcripts (β -actin, tubulin, and *MYC*).

141 We next sought to interrogate primary cancer samples to examine if a
142 correlation between *miR34a* asRNA and *miR34a* expression levels could be
143 identified. For this task we utilized RNA sequencing data from The Cancer
144 Genome Atlas (TCGA) after stratifying patients by cancer type, *TP53* status
145 and, where appropriate, cancer subtypes. The results indicate
146 that *miR34a* asRNA and *miR34a* expression are strongly correlated in the
147 vast majority of cancer types examined, both in the presence and absence of
148 wild-type *TP53* (**Fig. 1c, Supplementary Fig. 1a**). The results also further
149 confirm that the expression levels of both *miR34a* and its asRNA tend to be
150 reduced in patients with nonsynonymous *TP53* mutations.

151

152 Next, we aimed to gain a thorough understanding of *miR34a* asRNA's
153 molecular characteristics and cellular localization. Polyadenylation status was
154 evaluated via cDNA synthesis with either random nanomers or oligoDT
155 primers followed by semi-quantitative PCR with results indicating that
156 the *miR34a* asRNA is polyadenylated although the unspliced form seems to
157 only be in the polyA negative state (**Supplementary Fig. 1c**). To
158 experimentally determine the 3' termination site for the *miR34a* asRNA
159 transcript we performed 3' rapid amplification of cDNA ends (RACE) using the
160 U2OS osteosarcoma cell line that exhibited high endogenous levels
161 of *miR34a* asRNA in the cell panel screening. By sequencing the cloned
162 cDNA we determined that the transcripts 3' transcription termination site is
163 525 base pairs upstream of the *LINC01759* transcript's annotated termination
164 site (**Fig. 1d**). Next, we characterized the *miR34a* asRNA 5' transcription start
165 site by carrying out a primer walk assay, i.e. a common reverse primer was

166 placed in exon 2 and forward primers were gradually staggered upstream of
167 the transcripts annotated start site (**Supplementary Fig. 1b**). Our results
168 indicated that the 5' start site for *miR34a* asRNA is in fact approximately 90bp
169 (F11 primer) to 220bp (F12 primer) upstream of the annotated start site (**Fig.**
170 **1e**). We furthermore investigated the propensity of *miR34a* asRNA to be
171 alternatively spliced, using PCR cloning and sequencing and found that the
172 transcript is post-transcriptionally spliced to form multiple different isoforms
173 (**Supplementary Fig. 1d**). *make an additional supplementary figure showing
174 spliced RNAseq reads* Finally, to evaluate the cellular localization of miR34a
175 asRNA we utilized RNA sequencing data from five cancer cell lines included
176 in the ENCODE (Consortium 2012) project that had been fractionated into
177 cytosolic and nuclear fractions. The analysis revealed that the *miR34a* asRNA
178 transcript localizes to both the nucleus and cytoplasm but primarily resides in
179 the nucleus (**Supplementary Fig. 1f**).

180

181 Finally, we utilized multiple approaches to evaluate the coding potential of
182 the *miR34a* asRNA transcript. The Coding-Potential Assessment Tool is a
183 bioinformatics-based tool that uses a logistic regression model to evaluate
184 coding-potential by examining ORF length, ORF coverage, Fickett score and
185 hexamer score (Wang et al. 2013). Results indicated that *miR34a* asRNA has
186 a similar lack of coding capacity to the known non-coding
187 transcripts *HOTAIR* and *XIST* and differs greatly when examining these
188 parameters to the known coding transcripts β -actin, tubulin, and *MYC* (**Fig.**
189 **1F**). We further confirmed these results using the Coding-Potential Calculator
190 that utilizes a support based machine-based classifier and accesses an

191 alternate set of discriminatory features (**Supplementary Fig. 1E**) (Kong et al.
192 2007). *To fully evaluate coding potential methods such as mass
193 spectrometry or ribosome profiling must be used, however *miR34a* asRNA
194 presents little evidence of coding potential as evaluated by these two
195 bioinformatic approaches (31) [31]. We hope to be able to scan for peptides
196 matching to *miR34a* asRNA in TCGA before submission and, instead, will
197 mention results here....*

198

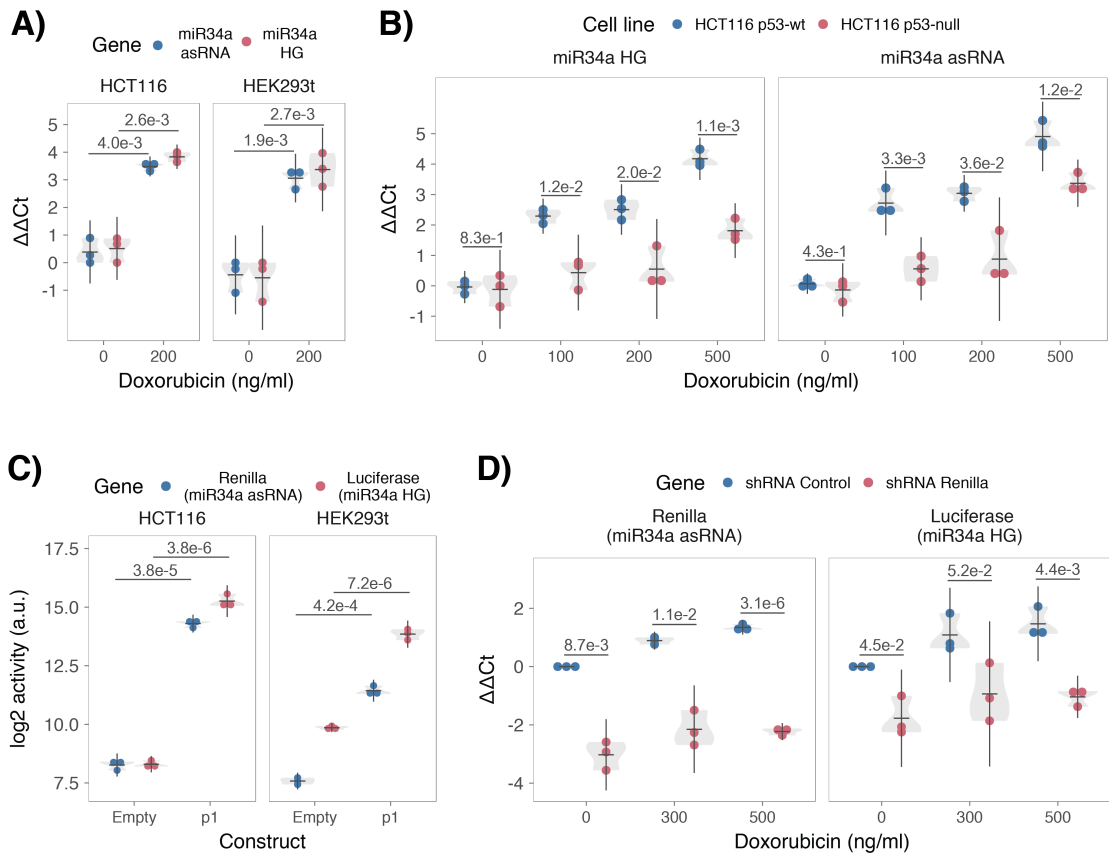
199 ***TP53-mediated regulation of miR34a asRNA expression***

200 *miR34a* is a known downstream target of TP53 and has been previously
201 shown to exhibit increased expression within multiple contexts of cellular
202 stress. *miR34a* asRNA has also been shown be induced upon TP53
203 activation in several global analyses of p53-regulated lncRNAs (Rashi-Elkeles
204 et al. 2014, Hunten et al. 2015, Leveille et al. 2015, Ashouri et al. 2016, Kim et
205 al. 2017). To confirm these results in our biological system, we treated
206 HEK293t, embryonic kidney cells, and HCT116, colorectal cancer cells, with
207 the DNA damaging agent doxorubicin to activate TP53. QPCR-mediated
208 measurement of both *miR34a* HG and asRNA indicated that their expression
209 levels were increased in response to doxorubicin treatment in both cell lines
210 (**Fig. 2a**). To assess if it is in fact *TP53* that is responsible for the increase
211 in *miR34a* asRNA expression upon DNA damage, we
212 treated *TP53^{+/+}* and *TP53^{-/-}* HCT116 cells with increasing concentrations of
213 doxorubicin and monitored the expression of both *miR34a* HG and asRNA.
214 We observed a dose-dependent increase in both *miR34a* HG and asRNA
215 expression levels with increasing amounts of doxorubicin, indicating that

216 these two transcripts are co-regulated, although, this effect was largely
217 abrogated in TP53^{-/-} cells (**Fig. 2b**). These results indicate
218 that *TP53* activation increases *miR34a* asRNA expression upon the induction
219 of DNA damage. Nevertheless, *TP53*^{-/-} cells also showed a dose dependent
220 increase in both *miR34a* HG and asRNA, indicating that additional factors,
221 other than *TP53*, are capable of initiating an increase in expression of both of
222 these transcripts upon DNA damage.

223

224



225 **Figure 2: TP53-mediated regulation of the *miR34a* locus.** **A)** Evaluating the effects of 24 hours of
 226 treatment with 200 ng/ml doxorubicin on *miR34a*asRNA and HG in HCT116 and HEK293t
 227 cells.* **B)** Monitoring *miR34a* HG and asRNA expression levels during 24 hours doxorubicin treatment
 228 in *TP53*^{+/+} and *TP53*^{-/-} HCT116 cells.* **C)** Quantification of luciferase and renilla levels after
 229 transfection of HCT116 and HEK293T cells with the p1 construct.* **D)** HCT116 cells were co-
 230 transfected with the p1 construct and shRNA renilla or shRNA control and subsequently treated with
 231 increasing doses of doxorubicin. 24 hours post-treatment, cells were harvested and renilla and
 232 luciferase levels were measured using QPCR. Resulting p-values from statistical testing are shown
 233 above the shRenilla samples which were compared to the shRNA control using the respective treatment
 234 condition.* *Individual points represent results from independent experiments and the gray shadow
 235 indicates the density of those points. Error bars show the 95% CI, black horizontal lines represent the
 236 mean, and p-values are shown over long horizontal lines indicating the comparison tested.
 237

238 The head-to head orientation of *miR34a* HG and asRNA, suggests that
239 transcription is initiated from a single promoter in a bi-directional manner. To
240 investigate whether *miR34a* HG and asRNA are transcribed from the same
241 promoter as divergent transcripts, we cloned the *miR34a* HG promoter,
242 including the *TP53* binding site, into a luciferase/renilla dual reporter vector
243 which we hereafter refer to as p1 (**Supplementary Fig. 2a and 2b**). Upon
244 transfection of p1 into HCT116 and HEK293t cell lines we observed increases
245 in both luciferase and renilla indicating that *miR34a* HG and asRNA
246 expression can be regulated by a single promoter contained within the p1
247 construct (**Fig. 2c**).

248

249 Although knock-down of endogenous *miR34a* asRNA is complicated due to its
250 various isoforms, we hypothesized that *miR34a* asRNA may
251 regulate *miR34a* HG levels and, in addition, that the overlapping regions of
252 the sense and antisense transcripts may have a crucial role in mediating this
253 regulation. Accordingly, we first co-transfected the p1 construct, containing
254 the overlapping region of the two transcripts, and a short hairpin (sh) RNA
255 targeting renilla into HCT116 cells subsequently treating them with increasing
256 doses doxorubicin. Analysis of luciferase and renilla expression revealed that
257 shRNA-mediated knock down of the renilla transcript (corresponding
258 to *miR34a* asRNA) caused luciferase (corresponding to *miR34a* HG) levels to
259 concomitantly decrease (**Fig. 2d**). This indicates that *miR34a* asRNA
260 positively regulates levels of *miR34a* HG and is crucial for an appropriate
261 TP53-mediated *miR34a* response to DNA damage. In addition, the results
262 show that the transcriptional product of the *miR34a* asRNA within in the p1

263 construct is necessary to elicit a miR34a response.

264

265 ***miR34a asRNA regulates its host gene independently of TP53***

266 Despite the fact that TP53 regulates *miR34a* HG and asRNA expression, our
267 results indicated that other factors are also able to regulate this locus (**Fig.**

268 **2b**). Utilizing a lentiviral system, we stably over-expressed the *miR34a* asRNA

269 transcript in three *TP53*-null cell lines; PC3 (prostate cancer), Saos2
270 (osteogenic sarcoma), and Skov3 (adenocarcinoma). We first analyzed the

271 levels of *miR34a* asRNA in these stable over-expression cell lines, compared

272 to HEK293T cells, which have high endogenous levels of *miR34a* asRNA,
273 finding that, on average, the over-expression was approximately 30-fold

274 higher in the over-expression cell lines than in HEK293t cells. Due to the fact

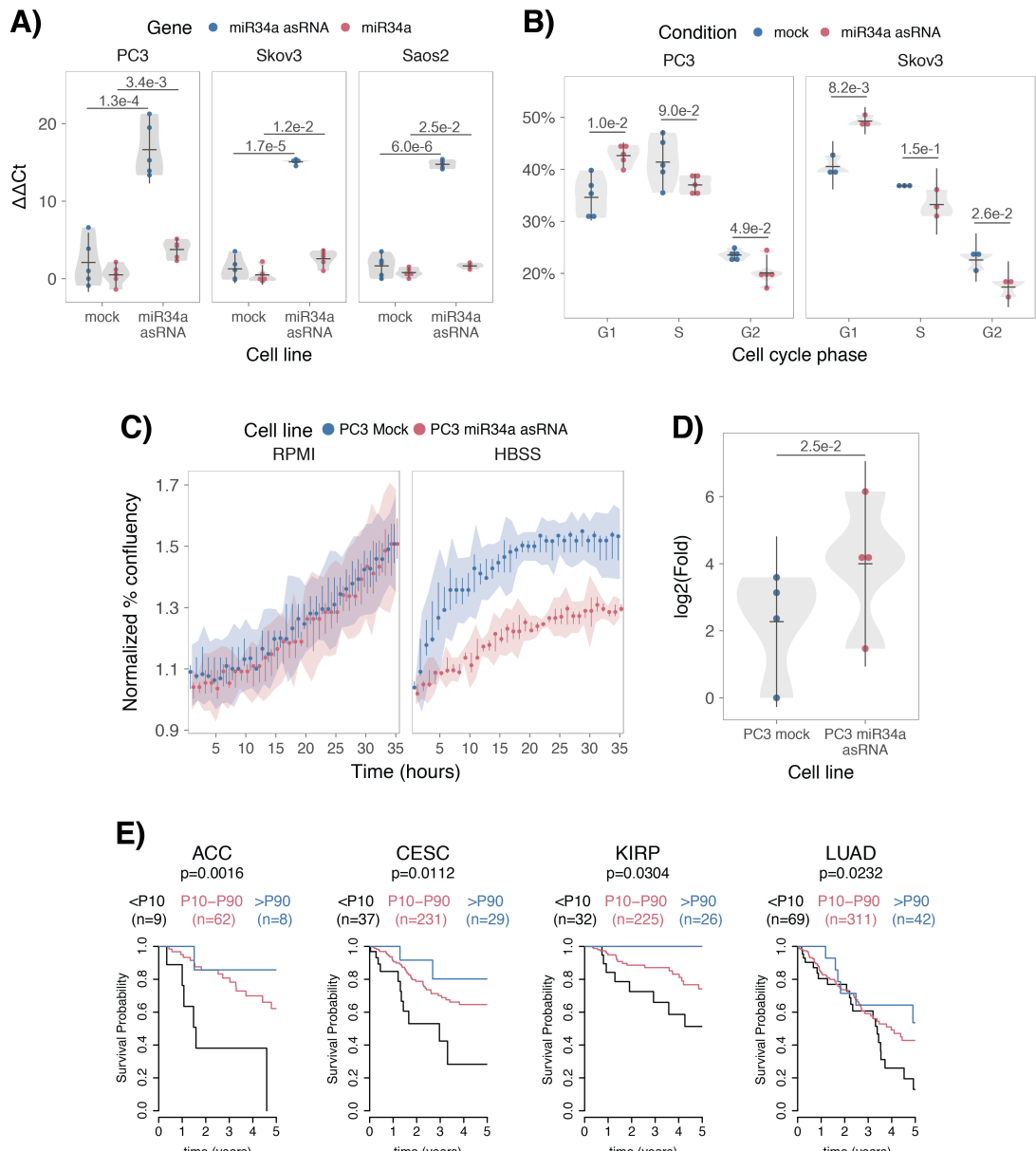
275 that *miR34a* asRNA can be up-regulated ~30-fold in response to DNA
276 damage (**Fig. 2b**), we deemed this over-expression level to correspond to

277 physiologically relevant levels in cells encountering a stress stimulus, such as
278 DNA damage (**Supplementary Fig. 3a**). Analysis of *miR34a* levels in

279 the *miR34a* asRNA over-expressing cell lines showed that *miR34a* asRNA
280 over-expression resulted in a concomitant increase in the expression

281 of *miR34a* in all three cell lines (**Fig. 3a**). These results indicate that, in the
282 absence of *TP53*, *miR34a* expression may be rescued by increasing the

283 levels of *miR34a* asRNA expression.



284

285 **Figure 3: miR34a asRNA positively regulates miR34a and its associated phenotypes.** A) QPCR-
286 mediated quantification of miR34a expression in cell lines stably over-
287 expressing miR34a asRNA.* B) Cell cycle analysis comparing stably over-expressing miR34a asRNA
288 cells to the respective mock expressing cells.* C) Analysis of cellular growth over time in miR34a
289 asRNA over-expressing PC3 cells. Points represent the median from 3 independent experiments, the
290 colored shadows indicate the 95% confidence interval, and vertical lines show the minimum and
291 maximum values obtained from the three biological replicates. D) Differential phosphorylated
292 polymerase II binding in miR34a asRNA over-expressing PC3 cells.* E) Survival analysis dependent
293 on miR34a asRNA expression levels using TCGA data. P10 = 10%, P10-P90 = 10%-90%, P90 = 90%.
294 Adrenocortical carcinoma (ACC), Cervical squamous cell carcinoma and endocervical adenocarcinoma
295 (CESC), Kidney renal papillary cell carcinoma (KIRP), Lung adenocarcinoma (LUAD). *Individual
296 points represent results from independent experiments and the gray shadow indicates the density of
297 those points. Error bars show the 95% CI, black horizontal lines represent the mean, and p-values are
298 shown over long horizontal lines indicating the comparison tested.
299

300 *miR34a* has been previously shown to regulate cell cycle progression, with
301 *miR34a* induction causing G1 arrest. Cell cycle analysis via determination of
302 DNA content showed a significant increase in G1 phase cells in the PC3 and
303 Skov3 *miR34a* asRNA over-expressing cell lines, indicative of G1 arrest, as
304 well as, a significant decrease of cells in G2 phase (**Fig. 3b**). *miR34a*'s effects
305 on the cell cycle are mediated by its ability to target cell cycle regulators such
306 as cyclin D1 (*CCND1*) (Sun et al. 2008). We therefore sought to determine if
307 the *miR34a* asRNA over-expressing cell lines exhibited effects on this
308 known *miR34a* target. Quantification of both *CCND1* RNA expression
309 (**Supplementary Fig. 3b**) and protein levels (**Supplementary Fig. 3c**) in the
310 PC3 *miR34a* asRNA over-expressing cell line showed a significant decrease
311 of *CCND1* levels compared to the mock control.

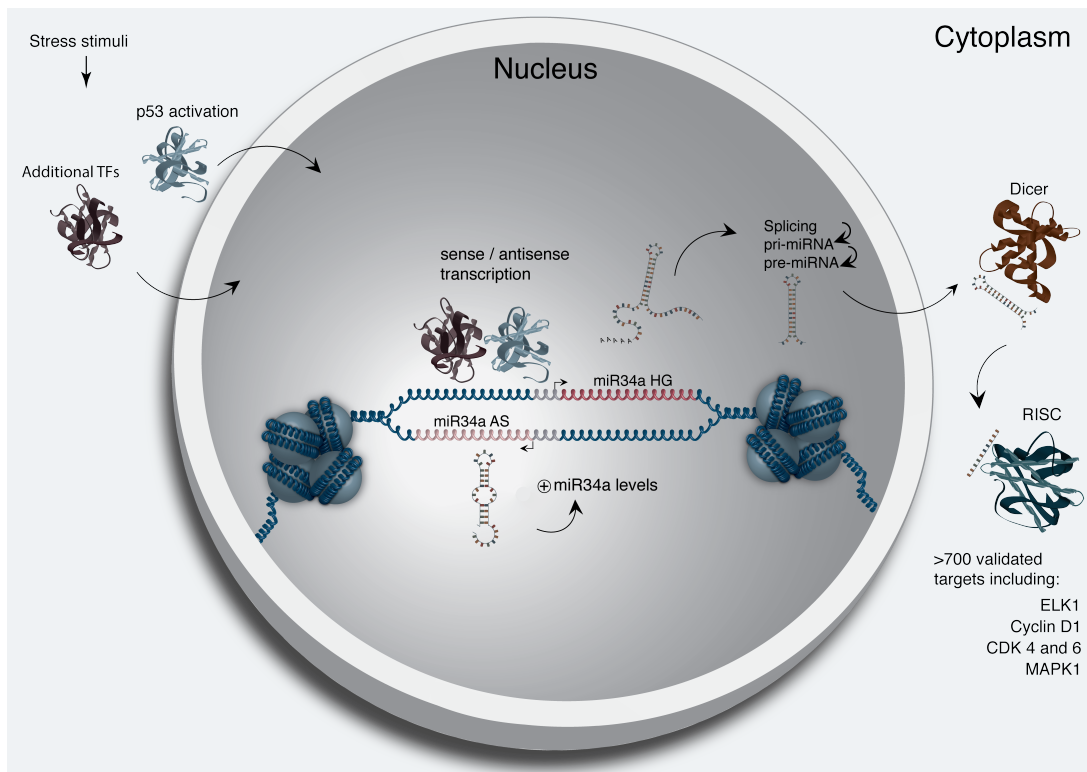
312
313 *miR34a* is also a well known inhibitor of cellular growth via its ability to
314 regulate growth factor signaling. Furthermore, starvation has been shown to
315 induce *miR34a* expression that down-regulates multiple targets that aid in the
316 phosphorylation of multiple pro-survival growth factors (Lal et al. 2011). We
317 further interrogated the effects of *miR34a* asRNA over-expression by
318 investigating the growth rate of the cells in both normal and starvation
319 conditions by measuring confluency over a 35-hour period. Although under
320 normal growth conditions there is only a marginal trend towards decreased
321 growth at individual early time points in *miR34a* asRNA over-expressing cell
322 lines, these effects on cell growth are drastically increased in starvation
323 conditions. This is in accordance with our previous results, and suggests
324 that *miR34a* asRNA-mediated increases in *miR34a* expression are crucial

325 under conditions of stress and necessary for the initiation of an appropriate
326 cellular response. In summary, we find that over-expression
327 of *miR34a* asRNA is sufficient to increase *miR34a* expression and gives rise
328 to known phenotypes observed with increased *miR34a* expression.

329

330 Antisense RNAs have been reported to mediate their effects both via
331 transcriptional and post-transcriptional mechanisms. Due to the fact that
332 *miR34a* expression is undetected in wild type PC3 cells but, upon over-
333 expression of *miR34a* asRNA, increases to detectable levels, we
334 hypothesized that *miR34a* asRNA is capable of regulating *miR34a* expression
335 levels via a transcriptional mechanism. To ascertain if this is actually the case,
336 we performed chromatin immunoprecipitation (ChIP) for phosphorylated
337 polymerase II (polII) at the *miR34a* HG promoter in both *miR34a* asRNA over-
338 expressing and mock control cell lines. Our results indicated a clear increase
339 in phosphorylated polII binding at the *miR34a* promoter upon *miR34a* asRNA
340 over-expression indicating *miR34a* asRNA's ability to regulate *miR34a* levels
341 on a transcriptional level (**Fig. 3d**).

342
343 *Finally, we investigated if *miR34a* asRNA levels affected the survival of
344 patients across a broad range of cancer types within the TCGA study. Of the
345 cancer types examined, we identified four where increased *miR34a* asRNA
346 levels gave rise to a beneficial prognosis (**Fig 3e**). This figure will either be
347 removed or modified before submission*



348

349 **Figure 4: A graphical summary of the proposed *miR34a* asRNA function.** Stress stimuli,
350 originating in the cytoplasm or nucleus, activates *TP53* as well as additional factors. These factors then
351 bind to the *miR34a* promoter and drive transcription of the sense and antisense strands. *miR34a* asRNA
352 serves to increase the levels of *miR34a* HG transcription via an unknown mechanism. *miR34a* HG
353 then, in turn, is then spliced, processed by the RNase III enzyme Drosha, and exported to the
354 cytoplasm. The *miR34a* pre-miRNA then binds to Dicer where the hair-pin loop is cleaved and
355 mature *miR34a* is formed. Binding of the mature *miR34a* miRNA to the RISC complex then allows it
356 to bind and repress its targets.
357 You can add polII in this figure

358 **Discussion**

359
360 Multiple studies have previously shown asRNAs to be crucial for the
361 appropriate regulation of cancer-associated protein-coding genes and that
362 their dys-regulation can lead to perturbation of tumor suppressive and
363 oncogenic pathways, as well as, cancer-related phenotypes (Yu et al. 2008,
364 Yap et al. 2010, Serviss et al. 2014, Balbin et al. 2015). Here we show that
365 asRNAs are also capable of regulating cancer-associated miRNAs resulting in
366 similar consequences as protein-coding gene dys-regulation (**Fig. 4**).
367 Interestingly, we show that, both in the presence and absence of
368 *TP53*, *miR34a* asRNA provides an additional regulatory level and functions by
369 mediating the increase of *miR34a* expression in both homeostasis and upon
370 encountering multiple forms of cellular stress. Furthermore, we find that
371 *miR34a* asRNA-mediated increases in *miR34a* expression levels are sufficient
372 to drive the appropriate cellular responses to multiple forms of stress stimuli
373 that are encountered (**Fig. 2d and Fig. 3c**). Previous studies have utilized
374 various molecular biology methods to up regulate *miR34a* expression in a p53
375 deficient background showing similar phenotypic outcomes but, to our
376 knowledge, this is the first example of an endogenous mechanism by which
377 this can be achieved (Liu et al. 2011, Ahn et al. 2012, Yang et al. 2012,
378 Stahlhut et al. 2015, Wang et al. 2015).

379

380 In agreement with previous studies, we demonstrate that upon encountering
381 various types of cellular stress, TP53 in concert with additional factors bind
382 and initiate transcription at the *miR34a* locus, thus increasing the levels of
383 *miR34a* and, in addition, *miR34a* asRNA. We hypothesize that *miR34a*

384 asRNA may form a positive feedback for *miR34a* expression whereby *miR34a*
385 serves as a scaffold for the recruitment of additional factors that
386 support the expression of *miR34a* and, thus, driving the cell towards a
387 reduction in growth factor signaling, senescence, and eventually apoptosis.
388 On the other hand, in cells without a functional *TP53*, other factors, which
389 typically act independently or in concert with *TP53*, may initiate transcription
390 of the *miR34a* locus. We believe that *miR34a* asRNA could potentially be
391 interacting directly with one of these additional factors and recruiting it to the
392 *miR34a* locus in order to drive *miR34a* transcription. This is especially
393 plausible due to the fact that, due to the head-to-head orientation of the
394 *miR34a* HG and asRNA, there is sequence complementarity between the
395 RNA and the promoter DNA. Previous reports have illustrated the ability of
396 asRNAs to form hybrid DNA:RNA R-loops and, thus, facilitate an open
397 chromatin structure and the transcription of the sense gene (Boque-Sastre et
398 al. 2015). Nevertheless, further work will need to be performed to ascertain if
399 this mechanism is utilized in the case of *miR34a* asRNA.

400

401 An unannotated transcript, *Lnc34a*, arising from the antisense orientation of
402 the *miR34a* locus and with a transcription start site >250 bp upstream of the
403 annotated *miR34a* asRNAs start site, has been previously reported in a study
404 examining colorectal cancer (Wang et al. 2016). Among the findings in Wang
405 et al. the authors discover that *Lnc34a* negatively regulates miR34a
406 expression via recruitment of *DNMT3a*, *PHB2*, and *HDAC1* to the *miR34a*
407 promoter. Although the *Lnc34a* and *miR34a* asRNA transcripts share some
408 sequence similarity, we believe them to be separate RNAs that are,

409 potentially, different isoforms of the same gene. Furthermore, *Lnc34a* may be
410 highly context dependent and potentially only expressed at biologically
411 significant levels in colon cancer stem cells, or other stem-like cells, in
412 agreement with the conclusions drawn in the paper. We thoroughly address
413 our reasons for these beliefs and give appropriate supporting evidence in
414 (**Supplementary Results 4**). The fact that *Lnc34a* and *miR34a* asRNA would
415 appear to have opposing roles in their regulation of *miR34a* further underlines
416 the complexity of the regulation at this locus.

417

418 The fact that the p1 construct only contains a small portion of the *miR34a*
419 asRNA transcript indicates that this portion is sufficient to give rise to at least
420 a partial *miR34a* inducing response thus providing a potential pathway
421 towards oligonucleotide-mediated therapies (**Fig 2d, Supplementary Fig. 2a-**
422 **2b**). In fact, clinical trials utilizing *miR34a* replacement therapy have
423 previously been conducted but, disappointingly, were terminated after adverse
424 side effects of an immunological nature were observed in several of the
425 patients (Slabakova et al. 2017). Although it is not presently clear if these side
426 effects were caused by *miR34a* or the liposomal carrier used to deliver the
427 miRNA, the multitude of evidence indicating *miR34a*'s crucial role in
428 oncogenesis still makes its therapeutic induction an interesting strategy for
429 therapy and needs further investigation.

430

431 In summary, our results indicate that *miR34a* asRNA is a vital player in the
432 regulation of *miR34a* and is especially important in contexts where cellular
433 stresses are encountered. Due to the fact that many of these stress stimuli

434 are strongly associated with cancer, we believe *miR34a* asRNA's ability to
435 fine-tune *miR34a* expression levels to be especially crucial in tumorigenesis.

436

437 **Materials and Methods**

438 **Cell Culture**

439 All cell lines were cultured at 5% CO₂ and 37° C with HEK293T, Saos2, and
440 Skov3 cells cultured in DMEM high glucose (Hyclone), HCT116 and U2OS
441 cells in McCoy's 5a (Life Technologies), and PC3 cells in RPMI (Hyclone) and
442 2 mM L-glutamine. All growth mediums were supplemented with 10% heat-
443 inactivated FBS and 50 µg/ml of streptomycin and 50 µg/ml of penicillin.

444

445 **Bioinformatics and Data Availability**

446 The USCS genome browser (Kent et al. 2002) was utilized for the
447 bioinformatic evaluation of antisense transcription utilizing the RefSeq
448 (O'Leary et al. 2016) gene annotation track.

449

450 All raw experimental data, code used for analysis, and supplementary
451 methods are available for review at ([Serviss 2017](#)) and are provided as an R
452 package. All analysis took place using the R statistical programming language
453 (Team 2017) using multiple external packages that are all documented in the
454 package associated with the article (Wilkins , Chang 2014, Wickham 2014,
455 Wickham 2016, Allaire et al. 2017, Arnold 2017, Wickham 2017, Wickham
456 2017, Wickham 2017, Xiao 2017, Xie 2017). The package facilitates
457 replication of the operating system and package versions used for the original
458 analysis, reproduction of each individual figure included in the article, and
459 easy review of the code used for all steps of the analysis, from raw-data to

460 figure.

461

462 **Coding Potential**

463 Protein-coding capacity was evaluated using the Coding-potential
464 Assessment Tool (Wang et al. 2013) and Coding-potential Calculator (Kong et
465 al. 2007) with default settings. Transcript sequences for use with Coding-
466 potential Assessment Tool were downloaded from the UCSC genome
467 browser using the Ensembl
468 accessions: *HOTAIR* (ENST00000455246), *XIST* (ENST00000429829), β-
469 actin (ENST00000331789), Tubulin (ENST00000427480),
470 and *MYC* (ENST00000377970). Transcript sequences for use with Coding-
471 potential Calculator were downloaded from the UCSC genome browser using
472 the following IDs: *HOTAIR* (uc031qho.1), β-actin (uc003sq.4).

473

474 **shRNAs**

475 shRNA-expressing constructs were cloned into the U6M2 construct using the
476 BgIII and KpnI restriction sites as previously described (Amarzguioui et al.
477 2005) (Amarzguioui et al. 2005). shRNA constructs were transfected using
478 Lipofectamine 2000 or 3000 (Life Technologies). The sequence targeting
479 renilla is as follows: AAT ACA CCG CGC TAC TGG C.

480

481 **Lentiviral Particle production, infection, and selection**

482 Lentivirus production was performed as previously described in (Turner et al.
483 2012). Briefly, HEK293T cells were transfected with viral and expression
484 constructs using Lipofectamine 2000 (Life Technologies), after which viral

485 supernatants were harvested 48 and 72 hours post-transfection. Viral
486 particles were concentrated using PEG-IT solution (Systems Biosciences)
487 according to the manufacturer's recommendations. HEK293T cells were used
488 for virus titration and GFP expression was evaluated 72hrs post-infection via
489 flow cytometry after which TU/ml was calculated.

490 **Add stable line infection/selection here and change heading**

491 **Western Blotting**

492 Samples were lysed in 50 mM Tris-HCl, pH 7.4, 1% NP-40, 150 mM NaCl, 1
493 mM EDTA, 1% glycerol, 100 µM vanadate, protease inhibitor cocktail and
494 PhosSTOP (Roche Diagnostics GmbH). Lysates were subjected to SDS-
495 PAGE and transferred to PVDF membranes. The proteins were detected by
496 western blot analysis by using an enhanced chemiluminescence system
497 (Western Lightning-ECL, PerkinElmer). Antibodies used were specific
498 for CCND1 (Cell Signaling, cat. no. 2926, 1:1000), and β-actin (Sigma-Aldrich,
499 cat. no. A5441, 1:5000). All western blot quantifications were performed using
500 ImageJ (Schneider et al. 2012).

501

502 **Generation of U6-expressed miR34a AS Lentiviral Constructs**

503 The U6 promoter was amplified from the U6M2 cloning plasmid (Amarzguioui
504 et al. 2005) and ligated into the Not1 restriction site of the pHIV7-IMPDH2
505 vector (Turner et al. 2012). miR43a asRNA was PCR amplified and
506 subsequently cloned into the Nhe1 and Pac1 restriction sites in the pHIV7-
507 IMPDH2-U6 plasmid.

508

509 **Promoter Activity**

510 Cells were co-transfected with the renilla/firefly bidirectional promoter
511 construct (Polson et al. 2011) and GFP by using Lipofectamine 2000 (Life
512 Technologies). The expression of GFP and luminescence was measured 24 h
513 post transfection by using the Dual-Glo Luciferase Assay System (Promega)
514 and detected by the GloMax-Multi+ Detection System (Promega). The
515 expression of luminescence was normalized to GFP.

516

517 **Flow Cytometry**

518 Cells were harvested, centrifuged and, either re-suspended in PBS, 5% FBS
519 and analyzed for GFP expression using the LSRII machine (BD Biosciences).

520

521 **RNA Extraction and cDNA Synthesis**

522 For downstream SYBR green applications, RNA was extracted using the
523 RNeasy mini kit (Qiagen) and subsequently treated with DNase (Ambion
524 Turbo DNA-free, Life Technologies). 500ng RNA was used for cDNA
525 synthesis using MuMLV (Life Technologies) and a 1:1 mix of oligo(dT) and
526 random nanomers.

527 For analysis of miRNA expression with Taqman, samples were isolated with
528 trizol (Life Technologies) and further processed with the miRNeasy kit
529 (Qiagen). cDNA synthesis was performed using the TaqMan MicroRNA
530 Reverse Transcription Kit (Life Technologies) using the corresponding oligos
531 according to the manufacturer's recommendations.

532

533 **QPCR and PCR**

534 PCR was performed using the KAPA2G fast mix (Kapa Biosystems) with

535 corresponding primers. QPCR was carried out using KAPA 2G SYBRGreen
536 (Kapa Biosystems) using the Applied Biosystems 7900HT machine with the
537 cycling conditions: 95 °C for 3 min, 95 °C for 3 s, 60 °C for 30 s.
538 QPCR for miRNA expression analysis was performed according to the
539 protocol for the TaqMan microRNA Assay kit (Life Technologies) with the
540 same cycling scheme as above. Primer and probe sets for TaqMan were also
541 purchased from Life Technologies (TaqMan® MicroRNA Assay, hsa-miR-34a,
542 human and Control miRNA Assay, RNU48, human).

543 **Primers for all PCR-based experiments are listed in Supplementary Table 1.**

544

545 **Bi-directional Promoter Cloning**

546 The overlapping region (p1) corresponds with the sequence previously
547 published as the TP53 binding site in (Raver-Shapira et al. 2007) which we
548 synthesized and cloned into the pLucRluc construct (Polson et al. 2011).

549

550 **Cell Cycle Distribution**

551 Cells were washed in PBS and fixed in 4% PFA at room temperature
552 overnight. PFA was removed, and cells were re-suspended in 95% EtOH. The
553 samples were then rehydrated in distilled water, stained with DAPI and
554 analyzed by flow cytometry on a LSRII (BD Biosciences) machine. Resulting
555 cell cycle phases were quantified using the ModFit software (Verity Software
556 House).

557

558 **3' Rapid Amplification of cDNA Ends**

559 3'-RACE was performed as described as previously in (Johnsson et al. 2013).

560 Briefly, U2OS cell RNA was polyA-tailed using yeast polyA polymerase after
561 which cDNA was synthesized using oligo(dT) primers. Nested-PCR was
562 performed first using a forward primer in miR34a asRNA exon 1 and a tailed
563 oligo(dT) primer followed by a second PCR using an alternate miR34a asRNA
564 exon 1 primer and a reverse primer binding to the tail of the previously used
565 oligo(dT) primer. PCR products were gel purified and cloned the Strata Clone
566 Kit (Agilent Technologies), and sequenced.

567

568 **Chromatin Immunoprecipitation**

569 The ChIP was performed as previously described in (Johnsson et al. 2013)
570 with the following modifications. Cells were crosslinked in 1% formaldehyde,
571 quenched with glycine (0.125M), and lysed in cell lysis buffer (5mM PIPES,
572 85mM KCL, 0.5% NP40, protease inhibitor) and, sonicated in (50mM TRIS-
573 HCL pH 8.0, 10mM EDTA, 1% SDS, protease inhibitor) using a Bioruptor
574 Sonicator (Diagenode). Samples were incubated over night at 4°C with
575 the *poll* antibody (Abcam: ab5095) and subsequently pulled down with
576 Salmon Sperm DNA/Protein A Agarose (Upstate/Millipore) beads. DNA was
577 eluted in Elution buffer (1% SDS, 100mM NaHCO3), followed by reverse
578 crosslinking, RNaseA and protease K treatment. The DNA was eluted using
579 Qiagen PCR purification kit.

580 **Confluency Analysis**

581 **Fill this in**

582 **Pharmacological Compounds**

583 Doxorubicin was purchased from Teva (cat. nr. 021361). **MPA here**

584

585 **CAGE Analysis**

586 All available CAGE data from the ENCODE project (Consortium 2012) for 36
587 cell lines was downloaded from the UCSC genome browser (Kent et al. 2002)
588 for genome version hg19. Of these, 28 cell lines had CAGE transcription start
589 sites (TSS) mapping to the plus strand of chromosome 1 and in regions
590 corresponding to 200 base pairs upstream of the *lnc34a* start site (9241796 -
591 200) and 200 base pairs upstream of the GENCODE
592 annotated *miR34a* asRNA start site (9242263 + 200). These cell lines
593 included: HFDPC, H1-hESC, HMEpC, HAoEC, HPIEpC, HSaVEC, GM12878,
594 hMSC-BM, HUVEC, AG04450, hMSC-UC, IMR90, NHDF, SK-N-SH_RA, BJ,
595 HOB, HPC-PL, HAoAF, NHEK, HVMF, HWP, MCF-7, HepG2, hMSC-AT,
596 NHEM.f_M2, SkMC, NHEM_M2, and HCH. In total 74 samples were included.
597 17 samples were polyA-, 47 samples were polyA+, and 10 samples were total
598 RNA. In addition, 34 samples were whole cell, 15 enriched for the cytosolic
599 fraction, 15 enriched for the nucleolus, and 15 enriched for the nucleus. All
600 CAGE transcription start sites were plotted and the RPKM of the individual
601 reads was used to colour each read to indicate their relative abundance. In
602 cases where CAGE TSS spanned identical regions, the RPMKs of the regions
603 were summed and represented as one CAGE TSS in the figure. In addition, a
604 density plot shows the distribution of the CAGE reads in the specified
605 interval.

606

607 **Splice Junction Analysis**

608 All available whole cell (i.e. non-fractionated) spliced read data originating
609 from the Cold Spring Harbor Lab in the ENCODE project (Consortium 2012)

610 for 38 cell lines was downloaded from the UCSC genome browser (Kent et al.
611 2002). Of these cell lines, 36 had spliced reads mapping to the plus strand of
612 chromosome 1 and in the region between the *lnc34a* start (9241796) and
613 transcription termination (9257102) site (note that *miR34a* asRNA resides
614 totally within this region). Splice junctions from the following cell lines were
615 included in the final figure: A549, Ag04450, Bj, CD20, CD34 mobilized,
616 Gm12878, H1hesc, Haoaf, Haoec, Hch, Helas3, Hepg2, Hfdpc, Hmec,
617 Hmepc, Hmscat, Hmscbm, Hmscuc, Hob, Hpcpl, Hpiepc, Hsavec, Hsmm,
618 Huvec, Hvmf, Hwp, Imr90, Mcf7, Monocd14, Nhdf, Nhek, Nhemfm2,
619 Nhemm2, Nhlf, Skmc, and Sknsh. All splice junctions were included in the
620 figure and coloured according to the number of reads corresponding to
621 each. In cases where identical reads were detected multiple times, the read
622 count was summed and represented as one read in the figure.

623

624 **Correlation analysis**

625 Erik/Jimmy should probably take this.

626

627 **Acknowledgments**

628

629 **Competing Interests**

630

631 The authors declare no competing interests.

632

633 **Figure Supplements**

634

635 List figure supplements here!

636

637 **Supplementary Figures**

638

639

A)

cancer	all n	all rho	all p	TP53wt n	TP53wt rho	TP53wt p	TP53mut n	TP53mut rho	TP53mut p
ACC	10	5.52e-01	1.04e-01	10	5.52e-01	1.04e-01	NA	NA	NA
BLCA	228	5.15e-01	7.89e-17	134	4.53e-01	3.86e-08	94	4.27e-01	1.73e-05
BRCA Basal	42	5.74e-01	9.54e-05	10	6.24e-01	6.02e-02	32	5.74e-01	7.41e-04
BRCA Her2	44	1.47e-01	3.39e-01	12	2.24e-01	4.85e-01	32	6.82e-02	7.10e-01
BRCA LumA	199	3.41e-01	8.22e-07	177	3.43e-01	2.96e-06	22	4.86e-01	2.31e-02
BRCA LumB	70	1.71e-01	1.57e-01	61	1.48e-01	2.53e-01	9	1.67e-01	6.78e-01
CESC	156	1.39e-01	8.37e-02	145	1.60e-01	5.45e-02	11	-4.55e-02	9.03e-01
HNSC	313	5.37e-01	8.38e-25	123	6.08e-01	0.00e+00	190	4.47e-01	9.68e-11
KICH	5	6.00e-01	3.50e-01	5	6.00e-01	3.50e-01	NA	NA	NA
KIRC	142	3.49e-01	2.06e-05	141	3.37e-01	4.41e-05	NA	NA	NA
KIRP	167	4.51e-01	9.16e-10	163	4.48e-01	2.04e-09	4	8.00e-01	3.33e-01
LGG	271	6.33e-01	9.92e-32	76	7.28e-01	0.00e+00	195	3.87e-01	2.26e-08
LIHC	153	5.63e-01	3.64e-14	114	5.16e-01	4.18e-09	39	4.55e-01	3.95e-03
LUAD	234	2.82e-01	1.15e-05	128	3.61e-01	2.87e-05	106	2.27e-01	1.91e-02
LUSC	139	2.29e-01	6.74e-03	42	4.17e-02	7.93e-01	97	3.29e-01	9.91e-04
OV	56	2.33e-01	8.37e-02	10	8.42e-01	4.46e-03	46	1.46e-01	3.31e-01
PRAD	413	4.66e-01	1.33e-23	375	4.59e-01	6.13e-21	38	4.50e-01	4.58e-03
SKCM	165	6.48e-01	5.43e-21	152	6.10e-01	7.85e-17	13	4.34e-01	1.40e-01
STAD	225	3.72e-01	8.23e-09	145	3.67e-01	5.71e-06	80	4.20e-01	1.03e-04
THCA	469	4.58e-01	1.07e-25	467	4.62e-01	4.06e-26	NA	NA	NA

640
641
642
643
644
645
646
647
648

Figure 1_Supplement 1: A) Spearman's rho and p-values (p) from the correlation analysis investigating the correlation between miR34a and miR34a asRNA expression in TP53 wild type (wt) and mutated (mut) samples within TCGA cancer types. Bladder Urothelial Carcinoma (BLCA), Breast invasive carcinoma (BRCA), Head and Neck squamous cell carcinoma (HNSC), Lower Grade Glioma (LGG), Liver hepatocellular carcinoma (LIHC), Lung adenocarcinoma (LUAD), Lung squamous cell carcinoma (LUSC), Ovarian serous cystadenocarcinoma (OV), Prostate adenocarcinoma (PRAD), Skin Cutaneous Melanoma (SKCM), Stomach adenocarcinoma (STAD).

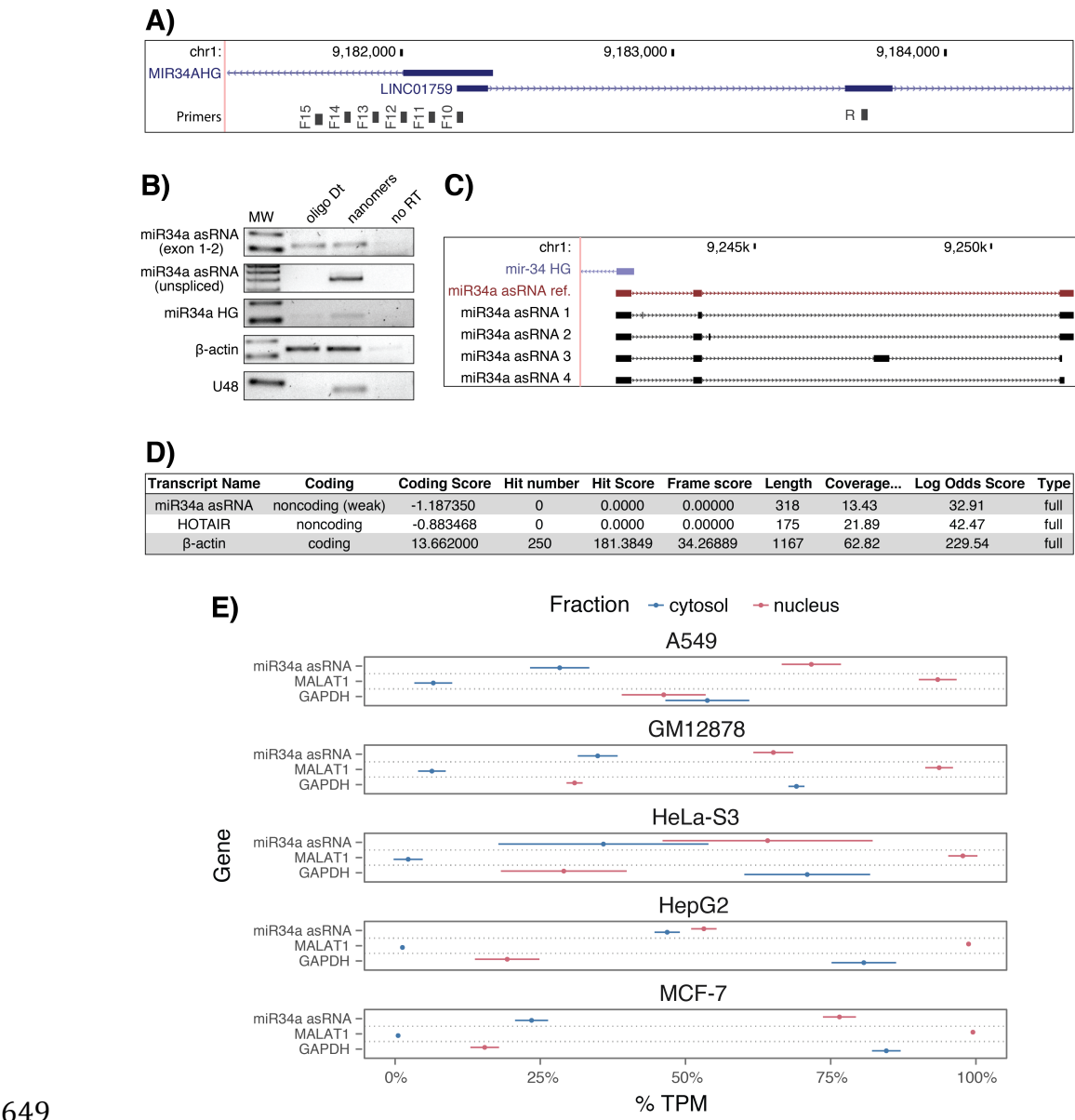
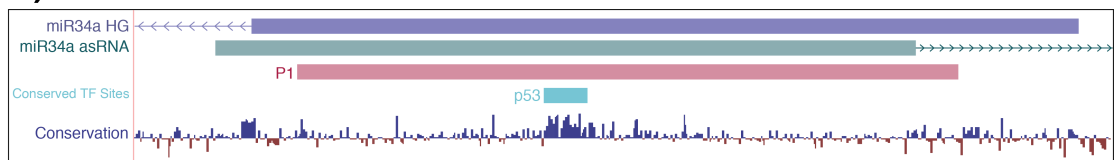


Figure 1 Supplement 2: **A)** A schematic representation of the primer placement in the primer walk assay. **B)** Polyadenylation status of spliced and unspliced miR34a asRNA in HEK293T cells. **C)** Sequencing results from the analysis of *miR34a* asRNA isoforms in U2OS cells. *miR34a* AS ref. refers to the full length transcript as defined by the 3'-RACE and primer walk assay. **D)** Analysis of coding potential of the *miR34a* asRNA transcript using the Coding-potential Calculator. **E)** RNAseq data from five fractionated cell lines in the ENCODE project showing the percentage of transcripts per million (TPM) for miR34a asRNA. MALAT1 (nuclear localization) and GAPDH (cytoplasmic localization) are included as fractionation controls. Points represent the mean and horizontal lines represent the standard deviation from two biological replicates.

A)



B)



661
662
663
664
665
666

Figure 2 Supplement 1: **A)** A UCSC genome browser illustration indicating the location of the promoter region cloned into the p1 construct including the conserved TP53-binding site. **B)** A representative picture of the p1 construct including forward (F) and reverse (R) primer locations and the renilla shRNA targeting site.

667
668
669
670
671
672

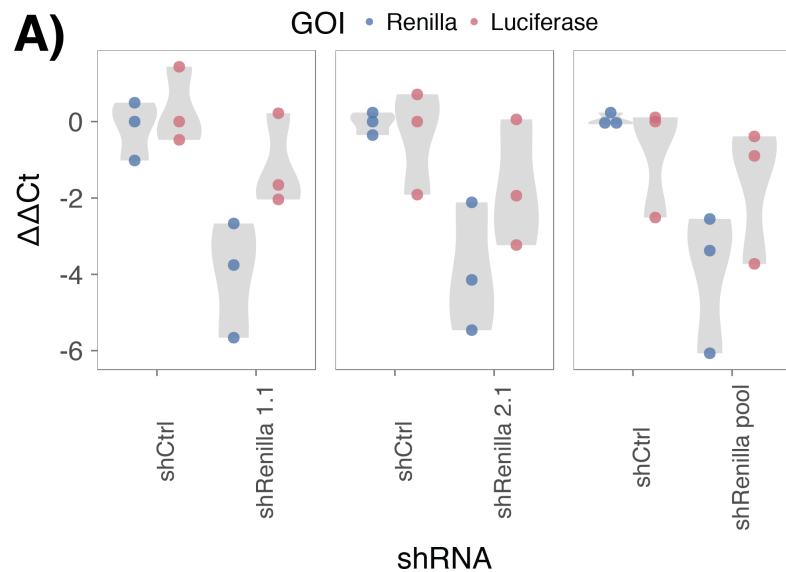
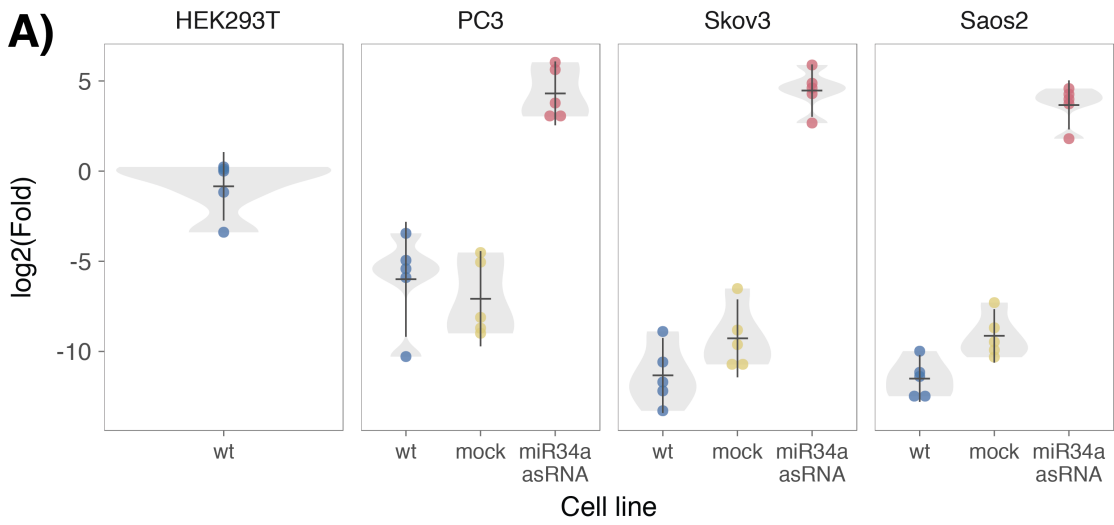


Figure 2 Supplement 2: A) HEK293T cells were co-transfected with the P1 construct and either shRenilla or shControl. Renilla and luciferase levels were measured with Q-PCR 48 hours after transfection. Individual points represent independent experiments with the gray shadow indicating the density of the points.



673
674
675
676
677

Figure 3 Supplement 1: A) Comparison of *miR34a* asRNA expression in HEK293T cells (high endogenous *miR34a* asRNA), and the wild-type (wt), mock, and *miR34a* over-expressing stable cell lines.

678
679
680
681

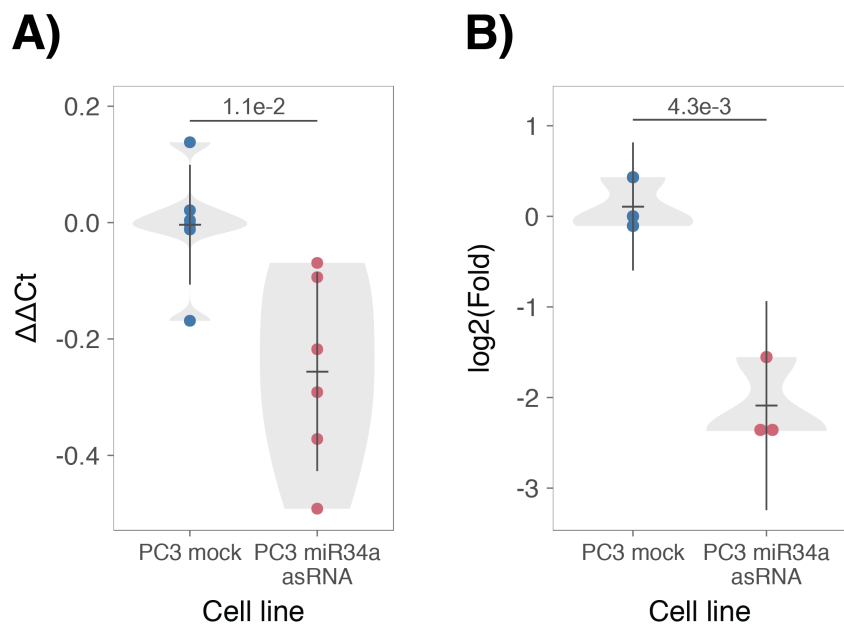
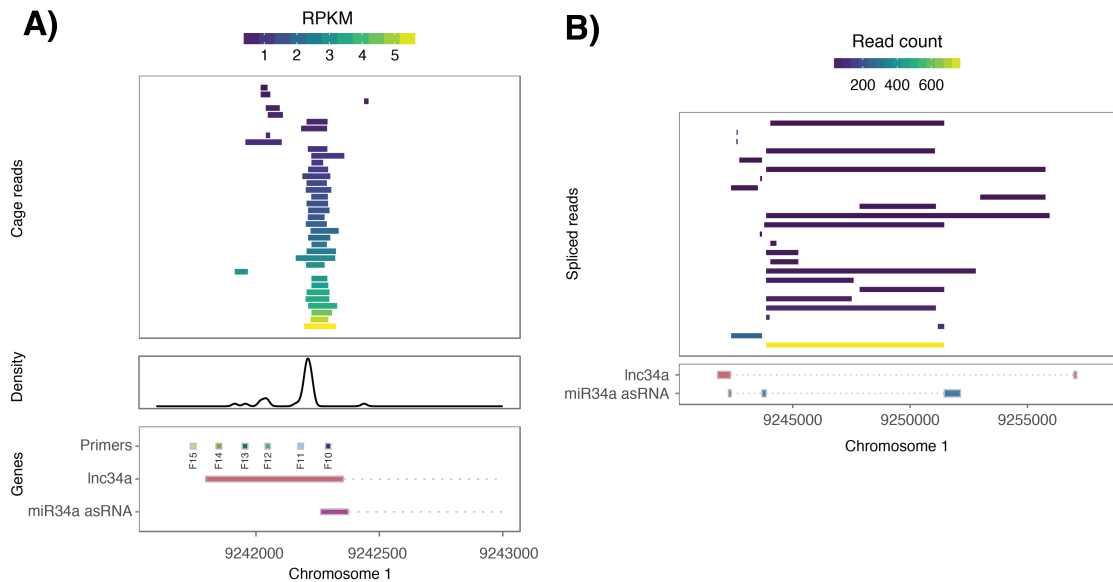


Figure 3 Supplement 2: CCND1 expression (A) and western blot quantification of protein levels (B) in *miR34a* asRNA over-expressing PC3 stable cell lines.



682
683
684
685
686
687
688
689
690
691

Supplementary Figure 4: A) CAGE transcription start sites from 28 ENCODE cell lines which mapped between 200 base pairs upstream of the *lnc34a* start site and 200 base pairs upstream of the GENCODE annotated *miR34a* asRNA start site (top panel). The density of the CAGE reads (middle panel) and the transcription start regions for *lnc34a* and the annotated *miR34a* asRNA, as well as, primer positions from the primer walk assay (bottom panel) are also illustrated. B) Spliced reads from 36 ENCODE cell lines which had reads mapping to the *lnc34a/miR34a* asRNA locus (top panel) and the *lnc34a* and *miR34a* asRNA genes (bottom panel).

692

693 **References**

694

695 Agostini, M., P. Tucci, R. Killick, E. Candi, B. S. Sayan, P. Rivetti di Val Cervo, P.
 696 Nicotera, F. McKeon, R. A. Knight, T. W. Mak and G. Melino (2011). "Neuronal
 697 differentiation by TAp73 is mediated by microRNA-34a regulation of synaptic
 698 protein targets." *Proc Natl Acad Sci U S A* **108**(52): 21093-21098. DOI:
 699 10.1073/pnas.1112061109

700

701 Ahn, Y. H., D. L. Gibbons, D. Chakravarti, C. J. Creighton, Z. H. Rizvi, H. P. Adams, A.
 702 Pertsemlidis, P. A. Gregory, J. A. Wright, G. J. Goodall, E. R. Flores and J. M. Kurie
 703 (2012). "ZEB1 drives prometastatic actin cytoskeletal remodeling by
 704 downregulating miR-34a expression." *J Clin Invest* **122**(9): 3170-3183. DOI:
 705 10.1172/JCI63608

706

707 Allaire, J., Y. Xie, J. McPherson, J. Luraschi, K. Ushey, A. Atkins, H. Wickham, J.
 708 Cheng and W. Chang (2017). rmarkdown: Dynamic Documents for R. R package
 709 version 1.8. <https://CRAN.R-project.org/package=rmarkdown>

710

711 Amarzguioui, M., J. J. Rossi and D. Kim (2005). "Approaches for chemically
 712 synthesized siRNA and vector-mediated RNAi." *FEBS Lett* **579**(26): 5974-5981.
 713 DOI: 10.1016/j.febslet.2005.08.070

714

715 Arnold, J. B. (2017). ggthemes: Extra Themes, Scales and Geoms for 'ggplot2'. R
 716 package version 3.4.0. <https://CRAN.R-project.org/package=ggthemes>

717

718 Ashouri, A., V. I. Sayin, J. Van den Eynden, S. X. Singh, T. Papagiannakopoulos and
 719 E. Larsson (2016). "Pan-cancer transcriptomic analysis associates long non-
 720 coding RNAs with key mutational driver events." *Nature Communications* **7**:
 721 13197. DOI: 10.1038/ncomms13197

722

723 Balbin, O. A., R. Malik, S. M. Dhanasekaran, J. R. Prensner, X. Cao, Y. M. Wu, D.
 724 Robinson, R. Wang, G. Chen, D. G. Beer, A. I. Nesvizhskii and A. M. Chinnaian
 725 (2015). "The landscape of antisense gene expression in human cancers." *Genome
 726 Res* **25**(7): 1068-1079. DOI: 10.1101/gr.180596.114

727

728 Boque-Sastre, R., M. Soler, C. Oliveira-Mateos, A. Portela, C. Moutinho, S. Sayols, A.
 729 Villanueva, M. Esteller and S. Guil (2015). "Head-to-head antisense transcription
 730 and R-loop formation promotes transcriptional activation." *Proc Natl Acad Sci U
 731 S A* **112**(18): 5785-5790. DOI: 10.1073/pnas.1421197112

732

733 Chang, T. C., D. Yu, Y. S. Lee, E. A. Wentzel, D. E. Arking, K. M. West, C. V. Dang, A.
 734 Thomas-Tikhonenko and J. T. Mendell (2008). "Widespread microRNA
 735 repression by Myc contributes to tumorigenesis." *Nat Genet* **40**(1): 43-50. DOI:
 736 10.1038/ng.2007.30

737

738 Chang, W. (2014). extrafont: Tools for using fonts. R package version 0.17.
 739 <https://CRAN.R-project.org/package=extrafont>

740

- 741 Chen, J., M. Sun, W. J. Kent, X. Huang, H. Xie, W. Wang, G. Zhou, R. Z. Shi and J. D.
742 Rowley (2004). "Over 20% of human transcripts might form sense-antisense
743 pairs." *Nucleic Acids Res* **32**(16): 4812-4820. DOI: 10.1093/nar/gkh818
- 744
- 745 Cheng, J., L. Zhou, Q. F. Xie, H. Y. Xie, X. Y. Wei, F. Gao, C. Y. Xing, X. Xu, L. J. Li and S.
746 S. Zheng (2010). "The impact of miR-34a on protein output in hepatocellular
747 carcinoma HepG2 cells." *Proteomics* **10**(8): 1557-1572. DOI:
748 10.1002/pmic.200900646
- 749
- 750 Chim, C. S., K. Y. Wong, Y. Qi, F. Loong, W. L. Lam, L. G. Wong, D. Y. Jin, J. F. Costello
751 and R. Liang (2010). "Epigenetic inactivation of the miR-34a in hematological
752 malignancies." *Carcinogenesis* **31**(4): 745-750. DOI: 10.1093/carcin/bgq033
- 753
- 754 Cole, K. A., E. F. Attiyeh, Y. P. Mosse, M. J. Laquaglia, S. J. Diskin, G. M. Brodeur and
755 J. M. Maris (2008). "A functional screen identifies miR-34a as a candidate
756 neuroblastoma tumor suppressor gene." *Mol Cancer Res* **6**(5): 735-742. DOI:
757 10.1158/1541-7786.MCR-07-2102
- 758
- 759 Conley, A. B. and I. K. Jordan (2012). "Epigenetic regulation of human cis-natural
760 antisense transcripts." *Nucleic Acids Res* **40**(4): 1438-1445. DOI:
761 10.1093/nar/gkr1010
- 762
- 763 Consortium, E. P. (2012). "An integrated encyclopedia of DNA elements in the
764 human genome." *Nature* **489**(7414): 57-74. DOI: 10.1038/nature11247
- 765
- 766 Ding, N., H. Wu, T. Tao and E. Peng (2017). "NEAT1 regulates cell proliferation
767 and apoptosis of ovarian cancer by miR-34a-5p/BCL2." *Onco Targets Ther* **10**:
768 4905-4915. DOI: 10.2147/OTT.S142446
- 769
- 770 Djebali, S., C. A. Davis, A. Merkel, A. Dobin, T. Lassmann, A. Mortazavi, A. Tanzer, J.
771 Lagarde, W. Lin, F. Schlesinger, C. Xue, G. K. Marinov, J. Khatun, B. A. Williams, C.
772 Zaleski, J. Rozowsky, M. Roder, F. Kokocinski, R. F. Abdelhamid, T. Alioto, I.
773 Antoshechkin, M. T. Baer, N. S. Bar, P. Batut, K. Bell, I. Bell, S. Chakrabortty, X.
774 Chen, J. Chrast, J. Curado, T. Derrien, J. Drenkow, E. Dumais, J. Dumais, R.
775 Duttagupta, E. Falconnet, M. Fastuca, K. Fejes-Toth, P. Ferreira, S. Foissac, M. J.
776 Fullwood, H. Gao, D. Gonzalez, A. Gordon, H. Gunawardena, C. Howald, S. Jha, R.
777 Johnson, P. Kapranov, B. King, C. Kingswood, O. J. Luo, E. Park, K. Persaud, J. B.
778 Preall, P. Ribeca, B. Risk, D. Robyr, M. Sammeth, L. Schaffer, L. H. See, A. Shahab, J.
779 Skancke, A. M. Suzuki, H. Takahashi, H. Tilgner, D. Trout, N. Walters, H. Wang, J.
780 Wrobel, Y. Yu, X. Ruan, Y. Hayashizaki, J. Harrow, M. Gerstein, T. Hubbard, A.
781 Reymond, S. E. Antonarakis, G. Hannon, M. C. Giddings, Y. Ruan, B. Wold, P.
782 Carninci, R. Guigo and T. R. Gingeras (2012). "Landscape of transcription in
783 human cells." *Nature* **489**(7414): 101-108. DOI: 10.1038/nature11233
- 784
- 785 Gallardo, E., A. Navarro, N. Vinolas, R. M. Marrades, T. Diaz, B. Gel, A. Quera, E.
786 Bandres, J. Garcia-Foncillas, J. Ramirez and M. Monzo (2009). "miR-34a as a
787 prognostic marker of relapse in surgically resected non-small-cell lung cancer."
788 *Carcinogenesis* **30**(11): 1903-1909. DOI: 10.1093/carcin/bgp219
- 789

- 790 Hunten, S., M. Kaller, F. Drepper, S. Oeljeklaus, T. Bonfert, F. Erhard, A. Dueck, N.
791 Eichner, C. C. Friedel, G. Meister, R. Zimmer, B. Warscheid and H. Hermeking
792 (2015). "p53-Regulated Networks of Protein, mRNA, miRNA, and lncRNA
793 Expression Revealed by Integrated Pulsed Stable Isotope Labeling With Amino
794 Acids in Cell Culture (pSILAC) and Next Generation Sequencing (NGS) Analyses."
795 Mol Cell Proteomics **14**(10): 2609-2629. DOI: 10.1074/mcp.M115.050237
- 796
- 797 International Human Genome Sequencing, C. (2004). "Finishing the euchromatic
798 sequence of the human genome." Nature **431**(7011): 931-945. DOI:
799 10.1038/nature03001
- 800
- 801 Johnsson, P., A. Ackley, L. Vidarsdottir, W. O. Lui, M. Corcoran, D. Grander and K.
802 V. Morris (2013). "A pseudogene long-noncoding-RNA network regulates PTEN
803 transcription and translation in human cells." Nat Struct Mol Biol **20**(4): 440-
804 446. DOI: 10.1038/nsmb.2516
- 805
- 806 Katayama, S., Y. Tomaru, T. Kasukawa, K. Waki, M. Nakanishi, M. Nakamura, H.
807 Nishida, C. C. Yap, M. Suzuki, J. Kawai, H. Suzuki, P. Carninci, Y. Hayashizaki, C.
808 Wells, M. Frith, T. Ravasi, K. C. Pang, J. Hallinan, J. Mattick, D. A. Hume, L. Lipovich,
809 S. Batalov, P. G. Engstrom, Y. Mizuno, M. A. Faghihi, A. Sandelin, A. M. Chalk, S.
810 Mottagui-Tabar, Z. Liang, B. Lenhard, C. Wahlestedt, R. G. E. R. Group, G. Genome
811 Science and F. Consortium (2005). "Antisense transcription in the mammalian
812 transcriptome." Science **309**(5740): 1564-1566. DOI: 10.1126/science.1112009
- 813
- 814 Kent, W. J., C. W. Sugnet, T. S. Furey, K. M. Roskin, T. H. Pringle, A. M. Zahler and D.
815 Haussler (2002). "The human genome browser at UCSC." Genome Res **12**(6):
816 996-1006. DOI: 10.1101/gr.229102. Article published online before print in May
817 2002
- 818
- 819 Kim, K. H., H. J. Kim and T. R. Lee (2017). "Epidermal long non-coding RNAs are
820 regulated by ultraviolet irradiation." Gene **637**: 196-202. DOI:
821 10.1016/j.gene.2017.09.043
- 822
- 823 Kong, L., Y. Zhang, Z. Q. Ye, X. Q. Liu, S. Q. Zhao, L. Wei and G. Gao (2007). "CPC:
824 assess the protein-coding potential of transcripts using sequence features and
825 support vector machine." Nucleic Acids Res **35**(Web Server issue): W345-349.
826 DOI: 10.1093/nar/gkm391
- 827
- 828 Lal, A., M. P. Thomas, G. Altschuler, F. Navarro, E. O'Day, X. L. Li, C. Concepcion, Y.
829 C. Han, J. Thiery, D. K. Rajani, A. Deutsch, O. Hofmann, A. Ventura, W. Hide and J.
830 Lieberman (2011). "Capture of microRNA-bound mRNAs identifies the tumor
831 suppressor miR-34a as a regulator of growth factor signaling." PLoS Genet **7**(11):
832 e1002363. DOI: 10.1371/journal.pgen.1002363
- 833
- 834 Leveille, N., C. A. Melo, K. Rooijers, A. Diaz-Lagares, S. A. Melo, G. Korkmaz, R.
835 Lopes, F. Akbari Moqadam, A. R. Maia, P. J. Wijchers, G. Geeven, M. L. den Boer, R.
836 Kalluri, W. de Laat, M. Esteller and R. Agami (2015). "Genome-wide profiling of
837 p53-regulated enhancer RNAs uncovers a subset of enhancers controlled by a
838 lncRNA." Nature Communications **6**: 6520. DOI: 10.1038/ncomms7520

- 839
840 Liu, C., K. Kelnar, B. Liu, X. Chen, T. Calhoun-Davis, H. Li, L. Patrawala, H. Yan, C.
841 Jeter, S. Honorio, J. F. Wiggins, A. G. Bader, R. Fagin, D. Brown and D. G. Tang
842 (2011). "The microRNA miR-34a inhibits prostate cancer stem cells and
843 metastasis by directly repressing CD44." *Nat Med* **17**(2): 211-215. DOI:
844 10.1038/nm.2284
- 845
846 Memczak, S., M. Jens, A. Elefsinioti, F. Torti, J. Krueger, A. Rybak, L. Maier, S. D.
847 Mackowiak, L. H. Gregersen, M. Munschauer, A. Loewer, U. Ziebold, M.
848 Landthaler, C. Kocks, F. le Noble and N. Rajewsky (2013). "Circular RNAs are a
849 large class of animal RNAs with regulatory potency." *Nature* **495**(7441): 333-
850 338. DOI: 10.1038/nature11928
- 851
852 O'Leary, N. A., M. W. Wright, J. R. Brister, S. Ciufo, D. Haddad, R. McVeigh, B.
853 Rajput, B. Robbertse, B. Smith-White, D. Ako-Adjei, A. Astashyn, A. Badretdin, Y.
854 Bao, O. Blinkova, V. Brover, V. Chetvernin, J. Choi, E. Cox, O. Ermolaeva, C. M.
855 Farrell, T. Goldfarb, T. Gupta, D. Haft, E. Hatcher, W. Hlavina, V. S. Joardar, V. K.
856 Kodali, W. Li, D. Maglott, P. Masterson, K. M. McGarvey, M. R. Murphy, K. O'Neill,
857 S. Pujar, S. H. Rangwala, D. Rausch, L. D. Riddick, C. Schoch, A. Shkeda, S. S. Storz,
858 H. Sun, F. Thibaud-Nissen, I. Tolstoy, R. E. Tully, A. R. Vatsan, C. Wallin, D. Webb,
859 W. Wu, M. J. Landrum, A. Kimchi, T. Tatusova, M. DiCuccio, P. Kitts, T. D. Murphy
860 and K. D. Pruitt (2016). "Reference sequence (RefSeq) database at NCBI: current
861 status, taxonomic expansion, and functional annotation." *Nucleic Acids Res*
862 **44**(D1): D733-745. DOI: 10.1093/nar/gkv1189
- 863
864 Ozsolak, F., P. Kapranov, S. Foissac, S. W. Kim, E. Fishilevich, A. P. Monaghan, B.
865 John and P. M. Milos (2010). "Comprehensive polyadenylation site maps in yeast
866 and human reveal pervasive alternative polyadenylation." *Cell* **143**(6): 1018-
867 1029. DOI: 10.1016/j.cell.2010.11.020
- 868
869 Polson, A., E. Durrett and D. Reisman (2011). "A bidirectional promoter reporter
870 vector for the analysis of the p53/WDR79 dual regulatory element." *Plasmid*
871 **66**(3): 169-179. DOI: 10.1016/j.plasmid.2011.08.004
- 872
873 Rashi-Elkeles, S., H. J. Warnatz, R. Elkon, A. Kupershtein, Y. Chobod, A. Paz, V.
874 Amstislavskiy, M. Sultan, H. Safer, W. Nietfeld, H. Lehrach, R. Shamir, M. L. Yaspo
875 and Y. Shiloh (2014). "Parallel profiling of the transcriptome, cistrome, and
876 epigenome in the cellular response to ionizing radiation." *Sci Signal* **7**(325): rs3.
877 DOI: 10.1126/scisignal.2005032
- 878
879 Raver-Shapira, N., E. Marciano, E. Meiri, Y. Spector, N. Rosenfeld, N. Moskovits, Z.
880 Bentwich and M. Oren (2007). "Transcriptional activation of miR-34a
881 contributes to p53-mediated apoptosis." *Mol Cell* **26**(5): 731-743. DOI:
882 10.1016/j.molcel.2007.05.017
- 883
884 Rinn, J. L., M. Kertesz, J. K. Wang, S. L. Squazzo, X. Xu, S. A. Brugmann, L. H.
885 Goodnough, J. A. Helms, P. J. Farnham, E. Segal and H. Y. Chang (2007).
886 "Functional demarcation of active and silent chromatin domains in human HOX

887 loci by noncoding RNAs." *Cell* **129**(7): 1311-1323. DOI:
888 10.1016/j.cell.2007.05.022
889
890 Rokavec, M., M. G. Oner, H. Li, R. Jackstadt, L. Jiang, D. Lodygin, M. Kaller, D. Horst,
891 P. K. Ziegler, S. Schwitalla, J. Slotta-Huspenina, F. G. Bader, F. R. Greten and H.
892 Hermeking (2015). "Corrigendum. IL-6R/STAT3/miR-34a feedback loop
893 promotes EMT-mediated colorectal cancer invasion and metastasis." *J Clin Invest*
894 **125**(3): 1362. DOI: 10.1172/JCI81340
895
896 Schneider, C. A., W. S. Rasband and K. W. Eliceiri (2012). "NIH Image to ImageJ:
897 25 years of image analysis." *Nat Methods* **9**(7): 671-675.
898
899 Serviss, J. T. (2017). miR34AasRNaproject.
900 https://github.com/GranderLab/miR34a_asRNA_project
901
902 Serviss, J. T., P. Johnsson and D. Grander (2014). "An emerging role for long non-
903 coding RNAs in cancer metastasis." *Front Genet* **5**: 234. DOI:
904 10.3389/fgene.2014.00234
905
906 Slabakova, E., Z. Culig, J. Remsik and K. Soucek (2017). "Alternative mechanisms
907 of miR-34a regulation in cancer." *Cell Death Dis* **8**(10): e3100. DOI:
908 10.1038/cddis.2017.495
909
910 Stahlhut, C. and F. J. Slack (2015). "Combinatorial Action of MicroRNAs let-7 and
911 miR-34 Effectively Synergizes with Erlotinib to Suppress Non-small Cell Lung
912 Cancer Cell Proliferation." *Cell Cycle* **14**(13): 2171-2180. DOI:
913 10.1080/15384101.2014.1003008
914
915 Su, X., D. Chakravarti, M. S. Cho, L. Liu, Y. J. Gi, Y. L. Lin, M. L. Leung, A. El-Naggar,
916 C. J. Creighton, M. B. Suraokar, I. Wistuba and E. R. Flores (2010). "TAp63
917 suppresses metastasis through coordinate regulation of Dicer and miRNAs."
918 *Nature* **467**(7318): 986-990. DOI: 10.1038/nature09459
919
920 Sun, F., H. Fu, Q. Liu, Y. Tie, J. Zhu, R. Xing, Z. Sun and X. Zheng (2008).
921 "Downregulation of CCND1 and CDK6 by miR-34a induces cell cycle arrest."
922 *FEBS Lett* **582**(10): 1564-1568. DOI: 10.1016/j.febslet.2008.03.057
923
924 Team, R. C. (2017). "R: A Language and Environment for Statistical Computing."
925 from <https://www.R-project.org/>.
926
927 Turner, A. M., A. M. Ackley, M. A. Matrone and K. V. Morris (2012).
928 "Characterization of an HIV-targeted transcriptional gene-silencing RNA in
929 primary cells." *Hum Gene Ther* **23**(5): 473-483. DOI: 10.1089/hum.2011.165
930
931 Vogt, M., J. Mundig, M. Gruner, S. T. Liffers, B. Verdoodt, J. Hauk, L.
932 Steinstraesser, A. Tannapfel and H. Hermeking (2011). "Frequent concomitant
933 inactivation of miR-34a and miR-34b/c by CpG methylation in colorectal,
934 pancreatic, mammary, ovarian, urothelial, and renal cell carcinomas and soft

935 tissue sarcomas." *Virchows Arch* **458**(3): 313-322. DOI: 10.1007/s00428-010-
936 1030-5
937
938 Wang, L., P. Bu, Y. Ai, T. Srinivasan, H. J. Chen, K. Xiang, S. M. Lipkin and X. Shen
939 (2016). "A long non-coding RNA targets microRNA miR-34a to regulate colon
940 cancer stem cell asymmetric division." *eLife* **5**. DOI: 10.7554/eLife.14620
941
942 Wang, L., H. J. Park, S. Dasari, S. Wang, J. P. Kocher and W. Li (2013). "CPAT:
943 Coding-Potential Assessment Tool using an alignment-free logistic regression
944 model." *Nucleic Acids Res* **41**(6): e74. DOI: 10.1093/nar/gkt006
945
946 Wang, X., J. Li, K. Dong, F. Lin, M. Long, Y. Ouyang, J. Wei, X. Chen, Y. Weng, T. He
947 and H. Zhang (2015). "Tumor suppressor miR-34a targets PD-L1 and functions
948 as a potential immunotherapeutic target in acute myeloid leukemia." *Cell Signal*
949 **27**(3): 443-452. DOI: 10.1016/j.cellsig.2014.12.003
950
951 Wickham, H. (2016). gtable: Arrange 'Grobs' in Tables. R package version 0.2.0.
952 <https://CRAN.R-project.org/package=gtable>
953
954 Wickham, H. (2017). scales: Scale Functions for Visualization. R package version
955 0.5.0. <https://CRAN.R-project.org/package=scales>
956
957 Wickham, H. (2017). tidyverse: Easily Install and Load the 'Tidyverse'. R package
958 version 1.2.1. <https://CRAN.R-project.org/package=tidyverse>
959
960 Wickham, L. H. a. H. (2017). rlang: Functions for Base Types and Core R and
961 'Tidyverse' Features. R package version 0.1.4. [https://CRAN.R-
962 project.org/package=rlang](https://CRAN.R-project.org/package=rlang)
963
964 Wickham, S. M. B. a. H. (2014). magrittr: A Forward-Pipe Operator for R. R
965 package version 1.5. <https://CRAN.R-project.org/package=magrittr>
966
967 Wilkins, D. ggenes: Draw Gene Arrow Maps in 'ggplot2'. R package version
968 0.2.0.9003. <https://github.com/wilkox/ggenes>
969
970 Xiao, N. (2017). liftr: Containerize R Markdown Documents. R package version
971 0.7. <https://CRAN.R-project.org/package=liftr>
972
973 Xie, Y. (2017). knitr: A General-Purpose Package for Dynamic Report Generation
974 in R. R package version 1.17. <https://yihui.name/knitr/>
975
976 Yang, P., Q. J. Li, Y. Feng, Y. Zhang, G. J. Markowitz, S. Ning, Y. Deng, J. Zhao, S.
977 Jiang, Y. Yuan, H. Y. Wang, S. Q. Cheng, D. Xie and X. F. Wang (2012). "TGF-beta-
978 miR-34a-CCL22 signaling-induced Treg cell recruitment promotes venous
979 metastases of HBV-positive hepatocellular carcinoma." *Cancer Cell* **22**(3): 291-
980 303. DOI: 10.1016/j.ccr.2012.07.023
981
982 Yap, K. L., S. Li, A. M. Munoz-Cabello, S. Raguz, L. Zeng, S. Mujtaba, J. Gil, M. J.
983 Walsh and M. M. Zhou (2010). "Molecular interplay of the noncoding RNA ANRIL

984 and methylated histone H3 lysine 27 by polycomb CBX7 in transcriptional
985 silencing of INK4a." Mol Cell **38**(5): 662-674. DOI: 10.1016/j.molcel.2010.03.021
986
987 Yu, W., D. Gius, P. Onyango, K. Muldoon-Jacobs, J. Karp, A. P. Feinberg and H. Cui
988 (2008). "Epigenetic silencing of tumour suppressor gene p15 by its antisense
989 RNA." Nature **451**(7175): 202-206. DOI: 10.1038/nature06468
990
991 Zenz, T., J. Mohr, E. Eldering, A. P. Kater, A. Buhler, D. Kienle, D. Winkler, J. Durig,
992 M. H. van Oers, D. Mertens, H. Dohner and S. Stilgenbauer (2009). "miR-34a as
993 part of the resistance network in chronic lymphocytic leukemia." Blood **113**(16):
994 3801-3808. DOI: 10.1182/blood-2008-08-172254
995
996